JAERI-M
91-132

HYDROGEN ABSORPTION BY ZIRCONIUM ALLOY CLADDING TUBE WITH SURFACE OXIDE FILM

August 1991

Masaaki UCHIDA

日本原子力研究所
Japan Atomic Energy Research Institute

JAERI-Mレポートは，日本原子力研究所が不定期に公刊している研究報告書です。
入手の問合わせは，日本原子力研究所技術情報部情報資料課（〒319-11茨城県那珂郡東海村）あて，お申しこしください。なお，このほかに財団法人原子力弘済会資料センター（〒319-11 茨城県那珂郡東海村日本原子力研究所内）で複写による実費頒布をおこなっております。

JAERI-M reports are issued irregularly.
Inquiries about availability of the reports should be addressed to Information Division, Department of Technical Information, Japan Atomic Energy Research Institute, Tokai-mura, Naka-gun, Ibaraki-ken 319-11, Japan.

編集兼発行　日本原子力研究所
印　　刷　㈱原子力資料サービス

JAERI-M 91-132

Hydrogen Absorption by Zirconium Alloy Cladding Tube with Surface Oxide Film

Masaaki UCHIDA

Department of Fuel Safety Research
Tokai Research Establishment
Japan Atomic Energy Research Institute
Tokai-mura, Naka-gun, Ibaraki-ken

(Received July 23, 1991)

Hydrogen absorption kinetics of Zircaloy (2 and 4) and Zr-Nb (1% and 2.5%) cladding tubes were studied by heating in hydrogen gas after oxide film formation in steam, oxygen or air. Hydrogen absorption rate depended on the degree of pre-oxidation. In Zr-Nb, the absorption rate was also sensitive to the atmosphere used for pre-oxidation, whereas in Zircaloy the rate was relatively independent of the kind of oxidant. In all materials, pre-oxidation to the transition point was found to bring about high absorption rate in the subsequent hydriding step. After pre-oxidation to the post-transition region, hydrogen absorption rate by Zircaloy showed constant or slightly decreasing tendency with increasing oxidation level, whereas in Zr-Nb, particularly in Zr-2.5%Nb, the rate showed a clearly decreasing tendency depending on the pre-oxidation atmosphere.

Different characteristics of Zircaloy and Zr-Nb can partly be explained in terms of different valencies of alloying elements which influence the lattice defect concentrations in the oxide films.

Keywords: Zirconium, Niobium, Zircaloy, Cladding, Oxide Film, Hydrogen, Corrosion

JAERI－M　91－132

酸化膜をつけたジルコニウム合金被覆管の水素吸収

日本原子力研究所東海研究所燃料安全工学部
内田　正明

(1991年7月23日受理)

酸化膜をつけたジルカロイ（2，4）およびZr－Nb（1％，2.5％）被覆管の水素吸収特性を，あらかじめ水蒸気または酸素または空気中で酸化した後，水素気体中で加熱する方法で調べた。一般に水素吸収速度は，酸化量に依存した。またZr－Nbでは，酸化時の雰囲気にも大きく依存したが，ジルカロイではあまり依存しなかった。いずれの材料も，酸化曲線の遷移点付近まで酸化した場合，水素吸収速度が大きくなる傾向がみられた。遷移点を越えて酸化した場合，ジルカロイの水素吸収速度は，酸化量によらずほぼ一定またはやや減少傾向を示した。Zr－Nb，特にZr－2.5 Nbでは遷移点を越えると，明かに水素吸収速度が低下する傾向を示した。ジルカロイとZr－Nbの特性の相違の一部は，合金元素の原子価の相違による酸化膜の欠陥濃度の相違によって説明できる。

東海研究所：〒319－11　茨城県那珂郡東海村白方字白根2－4

Contents

目　　次

1. Introduction

As higher burnup of light water reactor fuels is required, demands for new cladding material with higher corrosion resistance is increasing. High corrosion resistance here means not only small oxide growth rate; small absorption rate of the corrosion-product hydrogen can be even more important.

An important candidate material is zirconium-niobium alloy (Zr-Nb). Out of various Zr-Nb base alloys studied, only two alloys have actually been used in reactors: Zr-1%Nb is being used for cladding tubes in Russian water reactor fuels, and Zr-2.5%Nb is being used as pressure tube material in CANDU reactors.

Expectation to these alloys or new Nb-bearing Zr alloys comes mainly from the results of long-term out-pile corrosion experiments. In short-term tests, corrosion resistance of Zr-Nb alloys is no better than that of Zircaloys. As corrosion time is prolonged, however, oxidation curves for Zr-Nb alloys show greater saturating tendency than Zircaloys. Particularly, the transition phenomenon, enhancement of oxidation from 1/3th power dependence on time to linear kinetics known to occur in Zircaloys, has never been observed in Zr-Nb alloys during corrosion testing at realistic temperature, the longest record being 22000 hr at 350°C in Zr-1%Nb[1].

Concerning hydrogen pickup, Zr-Nb alloys are known for much smaller pick up ratio compared with that in Zircaloys. This difference is partly due to no occurence of transition in the Zr-Nb, because hydrogen pickup ratio is known to increase markedly with transition in zirconium and Zircaloys.

In reactor, however, corrosion of zirconium alloys generally proceeds faster than in out-pile tests. There, superiority of Zr-Nb to Zircaloys is not so clear as in out-pile test results. According to a review of the experiences of Zr-1%Nb in Russian LWRs by Hillner[2], although the alloy serves satisfactorily as cladding material, no evidence exists to show superiority of the alloy over Zircaloy. Vast experiences of Zr-2.5%Nb as pressure tube material in CANDU reactor cannot be used, because of the difference of temperature, to judge its corrosion resistance as cladding material. A comparative test of Zr-Nbs and Zircaloys in the NRU reactor[3] has shown that hydrogen pickup ratios by Zr-1%Nb and Zr-2.5%Nb are no less than that by Zircaloy-2

and 4.

Thus, at present there is no firm ground to believe that Zr-Nb or its modified alloys will show less corrosion rate nor less hydrogen pickup ratio than Zircaloys at long-term in-reactor service. If corrosion and hydrogen pickup behavior of Zr-Nb alloy during longer in-pile use is to be studied by out-pile tests, entire process must be accelerated and transition be realized by using high temperature steam. Corrosion test in high temperature steam were frequently performed in 1950's and 60's[4]-[7].

As an example of such tests, an experiment in 500°C steam by Rubel et al.[7] has shown that, although hydrogen pickup ratios by Zr-1%Nb and 2.5%Nb were smaller than that by Zircaloy-2 when compared at the same oxidation level, the ratio increased with transition to show a similar tendency as that of Zircaloy. However, this and similar experiments have never gone deep into the post-transition region: heating was interrupted soon after transition was observed. Since in-pile corrosion kinetics of zirconium alloys has a similarity to the post-transition kinetics in out-pile corrosion experiment, it is meaningful to add an experiment on hydrogen absorption through thick post-transition oxide films.

In the present experiment, oxidation and hydriding processes were separated into two successive steps. It is for limiting the use of high temperature for accelerating oxidation only, and studying the behavior of hydrogen at realistic cladding temperature. Experiments of this type, studying hydrogen absorption through pre-formed oxide film, have often been performed before 1960's[8].[9]. Since the objective of those experiments was a simulation of fuel failure due to hydrogen from fuel interior, the studied pre-formed oxide films were very thin. Hydrogen permeation through thick (post-transition) oxide film has never been studied.

Separation of oxidation and hydriding into two steps is of cource far from the simulation of the actual corrosion process in reactor fuels. However, it is also true that 'normal' type of out-pile corrosion experiments have not produced much information about the mechanism of hydrogen absorption. Even the kinetic informations have little applicability outside the boundary in which the experiment was performed. The present experiment aims at supplementing the knowledge about the hydrogen absorption process by zirconium alloy cladding

tubes by adopting a rather extreme experimental condition.

2. Experimental

The specimens were taken from cladding tubes of Zr-1%Nb, Zr-2.5%Nb, Zircaloy-2 and Zircaloy-4, all received in the unoxidized condition. They were used after cutting to 15-20 mm. Their dimensions, impurity contents and some mechanical properties are summarized in Table 1. Since these tubes were fabricated for use or testing in different reactor systems, they have considerably different diameters and wall thicknesses. The Zr-1%Nb tube which was fabricated for testing in ATR has the largest and the Zircaloy-4 tube for PWR has the smallest diameter. On the other hand, the Zr-2.5%Nb tube whose original purpose was a testing in CANDU reactor has a very small wall thickness relative to its diameter. To enable the comparison between these four specimens with different dimensions, kinetic data on oxidation and hydrogen absorption were both expressed as the amount of reaction (absorption) per surface area (mg/dm^2), in which surface area comprises inner, outer, and end faces.

Specimens after cutting were oxidized by heating either in steam (carried by argon), oxygen or atmospheric air. In either case, the oxidant was supplied sufficiently to sustain more than 10 times faster oxidation than actual. The oxidation temperature was changed between 400°C and 600°C depending on the target level of oxidation: most specimens for studying post-transition region were heated at 600°C. The specimens for low-level oxidation in air were anodized at two ends before heating to give additional protection (oxidation) there against excessive local hydriding in subsequent hydriding operation. But as this treatment turned out to be unnecessary for specimens oxidized to more than 50 mg/dm^2, it was skipped for high-level air-oxidation samples and all of the steam and oxygen oxidation samples.

Figure 1 shows the schematic of the hydriding apparatus. The cladding samples after oxidation (2 to 5 g each) were mounted into a quartz tube with an internal volume of 210 ml, and heated at 350°C evacuating the tube to less than 2×10^{-6} Torr and then filling with purified hydrogen gas to 1 atm. Before filling the tube, the impurity oxygen in the gas was removed by reaction with hydrogen to form water using palladium catalyst, and moisture was removed with silica-gel and

tubes by adopting a rather extreme experimental condition.

2. Experimental

The specimens were taken from cladding tubes of Zr-1%Nb, Zr-2.5%Nb, Zircaloy-2 and Zircaloy-4, all received in the unoxidized condition. They were used after cutting to 15-20 mm. Their dimensions, impurity contents and some mechanical properties are summarized in Table 1. Since these tubes were fabricated for use or testing in different reactor systems, they have considerably different diameters and wall thicknesses. The Zr-1%Nb tube which was fabricated for testing in ATR has the largest and the Zircaloy-4 tube for PWR has the smallest diameter. On the other hand, the Zr-2.5%Nb tube whose original purpose was a testing in CANDU reactor has a very small wall thickness relative to its diameter. To enable the comparison between these four specimens with different dimensions, kinetic data on oxidation and hydrogen absorption were both expressed as the amount of reaction (absorption) per surface area (mg/dm^2), in which surface area comprises inner, outer, and end faces.

Specimens after cutting were oxidized by heating either in steam (carried by argon), oxygen or atmospheric air. In either case, the oxidant was supplied sufficiently to sustain more than 10 times faster oxidation than actual. The oxidation temperature was changed between 400°C and 600°C depending on the target level of oxidation: most specimens for studying post-transition region were heated at 600°C. The specimens for low-level oxidation in air were anodized at two ends before heating to give additional protection (oxidation) there against excessive local hydriding in subsequent hydriding operation. But as this treatment turned out to be unnecessary for specimens oxidized to more than 50 mg/dm^2, it was skipped for high-level air-oxidation samples and all of the steam and oxygen oxidation samples.

Figure 1 shows the schematic of the hydriding apparatus. The cladding samples after oxidation (2 to 5 g each) were mounted into a quartz tube with an internal volume of 210 ml, and heated at 350°C evacuating the tube to less than 2×10^{-6} Torr and then filling with purified hydrogen gas to 1 atm. Before filling the tube, the impurity oxygen in the gas was removed by reaction with hydrogen to form water using palladium catalyst, and moisture was removed with silica-gel and

liquid nitrogen traps. After filling with hydrogen, the system was isolated by closing the valve and hydrogen absorption by the specimen was monitored in terms of gas pressure decrease measured by a diaphram-type pressure transducer.

Each hydriding run was continued for different lengths of time because, as stated later, hydrogen absorption rate varied quite extensively depending on material and the level of oxidation. Target hydriding level was generally set to be several hundred ppm. In some specimens, however, hydrogen absorption was null even after one week's heating while in others more than 1000 ppm hydrogen was absorbed in one hour. Some specimens were heated in hydrogen without pre-oxidation. In such runs, the hydrogen gas after purification was again parametrically contaminated before filling by mixing dry oxygen. It is for the purpose of studying a possible difference in the effects of simultaneous oxidation and pre-oxidation on hydriding.

The specimens before and after hydriding were weighed to an accuracy of 0.01 mg and the weight increase was compared with the amount of hydrogen absorption estimated from the pressure decrease data. In some specimens, absorbed hydrogen was extracted by evacuation at high temperature and analyzed by gas chromatography. Some of this analysis were made in two different states for a single specimen: one specimen after hydriding was cut to two pieces and one piece was analysed in this state and another one was analyzed after removal of oxide film with emery paper. Results of such analyses were used to estimate separate hydrogen contents in the metal and the oxide film.

Oxide films and hydride precipitation of some specimens were studied by metallography. X-ray diffraction study was also performed to characterize the oxide films.

3. Results

3.1 Oxidation

Oxidation kinetics (weight gain) of the four materials in three different atmospheres are illustrated in Figs. 2 to 4 as conventional log-log plots. Data points in these plots were taken from suvvessive weight increase data in several independent oxidation runs. Figures 2(a) and (b) show the oxidation curves in 500°C air of Zr-Nb and

liquid nitrogen traps. After filling with hydrogen, the system was isolated by closing the valve and hydrogen absorption by the specimen was monitored in terms of gas pressure decrease measured by a diaphram-type pressure transducer.

Each hydriding run was continued for different lengths of time because, as stated later, hydrogen absorption rate varied quite extensively depending on material and the level of oxidation. Target hydriding level was generally set to be several hundred ppm. In some specimens, however, hydrogen absorption was null even after one week's heating while in others more than 1000 ppm hydrogen was absorbed in one hour. Some specimens were heated in hydrogen without pre-oxidation. In such runs, the hydrogen gas after purification was again parametrically contaminated before filling by mixing dry oxygen. It is for the purpose of studying a possible difference in the effects of simultaneous oxidation and pre-oxidation on hydriding.

The specimens before and after hydriding were weighed to an accuracy of 0.01 mg and the weight increase was compared with the amount of hydrogen absorption estimated from the pressure decrease data. In some specimens, absorbed hydrogen was extracted by evacuation at high temperature and analyzed by gas chromatography. Some of this analysis were made in two different states for a single specimen: one specimen after hydriding was cut to two pieces and one piece was analysed in this state and another one was analyzed after removal of oxide film with emery paper. Results of such analyses were used to estimate separate hydrogen contents in the metal and the oxide film.

Oxide films and hydride precipitation of some specimens were studied by metallography. X-ray diffraction study was also performed to characterize the oxide films.

3. Results

3.1 Oxidation

Oxidation kinetics (weight gain) of the four materials in three different atmospheres are illustrated in Figs. 2 to 4 as conventional log-log plots. Data points in these plots were taken from suvvessive weight increase data in several independent oxidation runs. Figures 2(a) and (b) show the oxidation curves in 500°C air of Zr-Nb and

Zircaloys, respectively. Oxidation kinetics of either material showed an approximately 1/3th power time dependency until weight gain reached about 100 mg/dm^2. In this region, oxidation of Zircaloys proceeded at a rate a little smaller than that of Zr-Nbs. Then came a transition to a higher rate process, which correponded to a visual change of the oxide film from black to grey. After transition, oxidation rates of Zircaloys were larger than those of Zr-Nbs. In both pre-transition and post-transition regions, no systematic difference of oxidation rate was observed between two alloys in each group, i.e. between Zr-1%Nb and Zr-2.5%Nb, and between Zircaloy-2 and Zircaloy-4.

Figure 3(a) shows the oxidation kinetics of the four materials in steam at 500°C. In steam, the behaviors of Zr-Nb and Zircaloy groups were markedly different: Zircaloys showed a transition to a linear kinetics after 60 hrs at a weight gain of about 60 mg/dm^2, whereas the Zr-Nb group kept on the 1/3th power time dependency even after 500 hrs. To obtain steam-oxidized specimens, 600°C oxidation runs were added to the Zr-Nb groups and Zircaloy-4. Resultant oxidation curves are shown in Fig. 3(b). In this case, transition was observed above the oxidation level of about 200 mg/dm^2.

Figures 4(a) and (b) show the oxidation kinetics of the four materials in oxygen at 500°C and 600°C, respectively. In oxygen, no marked difference was observed between Zr-Nb and Zircaloy groups. Nor clear transition phenomenon was observed at 500°C even in Zircaloys. Consequently, oxidation rate of Zircaloys in the weight gain region of several hundred mg/dm^2 was smaller than that in steam. In contrast, oxidation rate in oxygen of Zr-Nbs was 2-3 times larger than in steam. At 600°C (Fig. 4(b)), fairly clear transition was observed especially in Zircaloys. These runs were interrupted at various levels of oxidation, and specimens with various oxide film thicknesses were subjected to hydriding operations.

3.2 Hydriding

In spite of pre-oxidation at different temperature, all hydriding runs were made at 350°C. The amount of absorbed hydrogen was estimated based mainly on the weight increase data, supplemented by gas pressure decrease and chemical analysis data. In specimens in which hydrogen was absorbed at moderate rates, the amounts determined by these three

methods agreed within a relative accuracy of ± 5%. After establishing this agreement and knowing the general dependency of hydrogen absorption on various factors, hydriding runs were often performed mounting several specimens in the apparatus simultaneously.

Typical examples of the hydrogen absorption kinetics for unoxidized or slightly oxidized specimens, as measured by pressure transducer, are shown in Fig. 5. With unoxidized surface, all four materials started hydrogen absorption readily after introduction of hydrogen gas and the hydrogen content reached several hundred ppm within one hour. To study the effect of oxidant content in the atmosphere on hydrogen absorption, oxygen was parametrically added to hydrogen and the resultant change in absorption rate was measured. Average absorption rate until hydrogen content reached 1000 ppm was taken as an index to describe the kinetics and plotted against oxygen content in the gas in Fig. 6. In the absence of gas analysis data, oxygen content in the purest gas was assumed arbitrarily to be 1 ppm; the actual content would have been smaller. Absorption rate is observed to decrease with increasing oxygen content in the ambient gas, especially above O_2/H_2 ratio of 10^{-4}. This dependency is in agreement with Boyle's observation that hydrogen absorption from gas phase is suppressed when, hydrogen contains more than 10^{-4} of moisture[10].

Hydrogen absorption kinetics of the spcimens alightly oxidized in air up to 50 mg/dm^2 generally followed either of the two typical patterns shown by the two curves in Fig. 5 for Zircaloy-2 and Zr-2.5%Nb. They are characterized by a sudden drop of pressure (rapid absorption) after a certain period of constant pressure (no absorption), which lasted in some cases for several days. Zircaloy-4 and Zr-1%Nb generally followed the same pattern as that shown by the example of Zircaloy-2 in Fig. 5. When carefully studied, it is observed that the kinetics of Zr-2.5%Nb is somewhat different from that of Zircaloy-2: although the sudden hydrogen absorption occured in Zr-2.5%Nb too, a period of slow but steady absorption preceded this 'catastrophic' absorption.

This sudden start of hydrogen absorption has been well known in old experiments. It has been correlated with the failure of reactor fuel due to contained moisture. This rapid absorption corresponds to breakdown of oxide film which starts generally at the cut ends of the tube specimens and propagates to side face as spallation of excessively

hydrided metal. However, it does not mean that this phenomenon is limited to specimens having sharply cut end faces. In fact, some specimens whose end faces were strengthened by anodizing before oxidation exhibited rapid absorption starting both from the end faces and side face simultaneously. Also, an example is reported in which the 'catastrophy' occured even in zirconium spheres, which naturally have no end faces[8].

The heating time in hydrogen elapsed before this 'catastrophy' in each run is plotted in Fig. 7 as a function of prior oxidation level. A tendency is observed that the occurence of this phenomenon is delayed as the level of pre-oxidation is increased. When oxidation level approached 50 mg/dm^2, examples as shown by upward arrows in Fig. 7 increased, which means that 'catastropy' was not observed within the limited heating time. In such specimens, hydrogen absorption proceeded nearly in proportion to time, or no absorption was observed at all. In either case, it was possible to define 'hydrogen absorption rate' deviding the weight increase by heating time.

The hydrogen absorption rates thus defined are plotted in Figs. 8 to 10, as a function of the prior oxidation level above 50 mg/dm^2, separately for the three defferent oxidation atmospheres. Different from the case of oixdation kinetics, run-to-run scattering in the hydriding rate was very large even under nominally identical conditions. This situation made it impossible to describe the effects of different materials and different pre-oxidation atmopsheres as something more than general tendencies.

Figure 8 shows the hydrogen absorption rates of the four materials at 350°C from 1 atmosphere pure hydrogen as a function of prior oxidation level in air at 500°C. Zircaloy-2 and -4 showed similar absorption rates, which were nearly constant over the pre-oxidation levels studied. In these two alloys, run-to-run scatter of the kinetic data was fairly small. In contrast, Zr-Nb alloys, especially Zr-2.5%Nb, showed a large scatter in absorption rate. It often occurred that some specimens absorbed hydrogen comparably with Zircaloys while similar specimens absorbed no detectable amount of hydrogen at all. When seen as a whole, however, hydrogen absorption rate by Zr-Nbs seems to increase to a level comparable to that by Zircaloys at the pre-oxidation level of 100-200 mg/dm^2, which roughly corresponds to transition point of oxidation kinetics, and then to decrease at higher oxidation levels.

Figure 9 is a similar plot for the specimens oxidized in steam. In this case, Zr-Nb specimens were pre-oxidized either at 500°C (small symbols) or 600°C (large symbols). The data points were so arranged that the specimens with the two different pre-treatments may overlap in the same oxidation level. Effect of different pre-oxidation temperature does not seem to exist. When pre-oxidation was made in steam, it was shown by chemical analysis that considerable amount of hydrogen was absorbed already during the oxidation step, particularly when oxidation was made beyond the transition point. The absorption rates in Fig. 9 stands only for the part absorbed during the hydriding step. As far as this part of absorption is considered, the dependency of the rate on the prior oxidation level is similar to the case of air-oxidized specimens. The absolute level of the absorption rate was, however, larger than the case of air-oxidized specimens, particularly in Zr-Nb alloys.

Figure 10 shows the case of speicmens oxidized in oxygen and then hydrided. In this case, 'catastrophic' absorption (indicated by the upward arrows in the figure) was observed even after pre-oxidation to a level as high as 200 mg/dm^2. The solid and broken lines in the figure were drawn for Zr-Nbs and Zircaloys, respectively, neglecting these runs as exceptional cases. As long as the data points described by these lines are concerned, hydrogen absorption rate by Zircaloy group seems to depend on the prior oxidation level in a similar way to the former two cases, i.e. constant or slightly decreasing absorption rate with oxidation level. On the other hand, the behavior of Zr-Nb group was markedly different from the cases of air- or steam-oxidized specimens. The solid line in Fig. 10 for Zr-Nb shows monotonously increasing tendency with prior oxidation level, exceeding the rates for the Zircaloy group at the highest oxidation level studied.

3.3 Metallography and X-ray diffraction

Some of the specimens after hudriding were metallographically examined for hydride precipitation and the pattern of oxide films. Since cut tube specimens were used in the present experiment, oxidation and hydriding proceeded both from the inner and outer surfaces. Though oxide film was a little thicker on the outer surface and hydrides were a little more densely precipitated near the inner surface, difference was small. Figure 11 shows photomicrographs (taken after hydriding) of

oxide films grown in steam on the outer surfaces of Zr-1%Nb, 2.5%Nb and Zircaloy-4 tube specimens. These oxide films were so brittle containing many cracks that polishing without spallation was almost impossible. At least in the optical microscopic level, no difference was evident between the films on Zr-Nb alloys and those on Zircaloys, nor between the films grown in different atmospheres.

Figure 12 shows examples of hydride precipitation in Zr-Nbs and Zircaloy-4. Though these examples represent the specimens oxidized in oxygen, the precipitation patterns in specimens oxidized in other atmospheres were again similar. Nor observed was much difference between Zr-Nbs and Zircaloys.

X-ray diffraction study was made on the oxide films formed under various conditions. Although complete study was not made on all combinations of experimental parameters, the parameters studied included different starting materials, different degrees of oxidation, before and after hydriding, and inner and outer surfaces of a tube specimen. Under the poor resolution of diffractions from curved surfaces, however, the only meaningful difference was observed to come from the difference in the oxidation level; all materials have given essentially the same diffraction pattern under the same oxidation level.

Typical examples of diffraction pattern from thin and thick oxide films are shown in Fig. 13(a) and (b), respectively. The oxide film for the pattern in Fig. 13(a) had a thickness of only about 1 μm. Peaks corresponding to both tetragonal and monoclinic ZrO_2 are visible. Zr and hydride peaks are considered to have originated from the underlying metal phase penetrating the thin oxide film. On the other hand, for thick oxide in Fig. 13(b), all peaks were identified as diffractions from monoclinic ZrO_2 except one peak which appears at $2\theta = 35.7°$ (for Cu Kα). It could not be identified as a diffraction from any oxide nor hydride nor metal phase of Zr and Nb.

3.4 Other observations

In the cource of experiment, some specimens were found to show an unexpected weight decrease during storage at room temperature either after oxidation or hydriding. Some examples of this process are shown in Fig. 14. This weight reduction generally continued for several days and stabilized within one week after dismantling from the furnace.

Since the reduction was rapid in the beginning and the first weighing had to be made after enough cooling of the specimen, the actual weight reduction would have been even greater than the data of Fig. 14 indicate.

As this weight reduction was evident in heavily oxidized specimens, the relative reduction until stabilization was plotted as a function of pre-oxidation level in Fig. 14. It is obvious that the reduction is related to oxidation beyond transition point. In this plot, Zr-2.5%Nb shows the greatest reduction among the four materials. It is, however, merely a result of expressing the amount of reduction as a fraction to total specimen weight which results in large value in thin-walled Zr-2.5%Nb tube. If the reduction is expressed as a value per unit surface area, difference between four materials is small.

This phenomenon is considered to be due to release of a part of hydrogen which existed in the oxide during oxidation or hydriding. To further investigate it, selected specimens after oxidation-hydriding were chemically analyzed for hydrogen such that the hydrogen atoms existing in the oxide and those in the metal could be separately determined. The specimens listed in Table 2 were symmetrically split into two pieces and they were analyzed, one after removal of oxide film using emery paper and another without removal. In fact, the oxide films were so hard that it was impossible to remove the oxide alone; some outer part of the metal was removed together.

Each analysis result in the Table represents an average of two to four independent operations. Local scatter was, however, very small. The data in Table 2 are taken to show that, if the value for the 'with oxide' specimen is higher, hydrogen concentration in the oxide is higher than in the metal, and if the 'without oxide' value is higher, hydrogen exists mainly in the metal. It is difficult to decide which level of difference is meaningful. Also, the number of data is too small for the variety of material, oxidation atmosphere and the levels of oxidation and hydriding.

With these limitations in mind, a general tendency is observed that partition of hydrogen between oxide film and the metal in Zr-Nb alloys is determined by the amount of hydrogen absorbed from gaseous hydrogen. Two Zr-1%Nb specimens N1-76 and N1-85 which have absorbed about 1000 ppm hydrogen during hydriding step show obviously higher concentration in the oxide film. Assuming that these two specimens had

uniform hydrogen concentration in the metal, H/O atom ratio in the oxide films in the two specimens are roughly calculated to be 1.6 and 0.7, respectively. On the other hand, Zr-2.5%Nb specimen N5-103 whose absorption during hydriding step was almost zero shows higher hydrogen concentration after removal of oxide film, suggesting that hydrogen in this sample (absorbed during oxidation step) existed in the metal. In Zircaloy-4 sample Y4-72 whose high hydrogen content comes mainly from absorption during oxidation step, hydrogen concentration after removal of oxide film is slightly higher.

It is difficult to draw a consistent picture on the partition of hydrogen between the metal and oxide in different materials after different treatments. It however seems certain, at least in Zr-Nb alloys, that high hydrogen permeability of oxide film (as indicated by large absorption value during hydriding step) is related to high concentration of hydrogen in the oxide.

4. Discussion

The present experiment was conducted separating oxidation and hydriding into two steps, which actually proceed simultaneously. This unusual experimental condition was inevitable if hydrogen pickup across thick oxide film on Zr-Nb alloy were to be studied in a relatively short period, limiting the use of high temperature only for acceleration of oxidation, not for hydriding. This sequence of experiment, however, contributed extensive scatter in the hydrogen absorption rate data, which made it difficult to make any definate statement on the effects of various factors.

Among the observed tendencies, the most obvious one will be that rate transition in oxidation generally results in high hydrogen absorption rate in all materials. This fact itself is a well-known phenomenon. As for the difference between Zr-Nb and Zircaloys, important points are 1)(in the post -transition region) Zr-Nbs show generally smaller hydrogen absorption rates than Zircaloys, 2) their hydriding rates are more dependent on the atmosphere at pre-oxidation, and 3) the scatter of absorption rate data is also greater.

High hydrogen absorption rate at transition will be related to the breakdown of the oxide film with phase change. The present X-ray diffraction study has shown that pre-transition oxide film consists of

uniform hydrogen concentration in the metal, H/O atom ratio in the oxide films in the two specimens are roughly calculated to be 1.6 and 0.7, respectively. On the other hand, Zr-2.5%Nb specimen N5-103 whose absorption during hydriding step was almost zero shows higher hydrogen concentration after removal of oxide film, suggesting that hydrogen in this sample (absorbed during oxidation step) existed in the metal. In Zircaloy-4 sample Y4-72 whose high hydrogen content comes mainly from absorption during oxidation step, hydrogen concentration after removal of oxide film is slightly higher.

It is difficult to draw a consistent picture on the partition of hydrogen between the metal and oxide in different materials after different treatments. It however seems certain, at least in Zr-Nb alloys, that high hydrogen permeability of oxide film (as indicated by large absorption value during hydriding step) is related to high concentration of hydrogen in the oxide.

4. Discussion

The present experiment was conducted separating oxidation and hydriding into two steps, which actually proceed simultaneously. This unusual experimental condition was inevitable if hydrogen pickup across thick oxide film on Zr-Nb alloy were to be studied in a relatively short period, limiting the use of high temperature only for acceleration of oxidation, not for hydriding. This sequence of experiment, however, contributed extensive scatter in the hydrogen absorption rate data, which made it difficult to make any definate statement on the effects of various factors.

Among the observed tendencies, the most obvious one will be that rate transition in oxidation generally results in high hydrogen absorption rate in all materials. This fact itself is a well-known phenomenon. As for the difference between Zr-Nb and Zircaloys, important points are 1)(in the post -transition region) Zr-Nbs show generally smaller hydrogen absorption rates than Zircaloys, 2) their hydriding rates are more dependent on the atmosphere at pre-oxidation, and 3) the scatter of absorption rate data is also greater.

High hydrogen absorption rate at transition will be related to the breakdown of the oxide film with phase change. The present X-ray diffraction study has shown that pre-transition oxide film consists of

a mixture of tetragonal and monoclinic ZrO_2 and post-transition one consists of monoclinic phase. It is in agreement with general knowledge on the transition phenomenon. Godlewski et al.[11] have shown by Raman spectroscopy of the oxide films of Zr-1%Nb and Zircaloy-4 that a layer containing 15 % tetragonal phase which is the principal pre-transition oxide structure forms an inner structure of the film even after transition.

On the other hand, Garzarolli et al.[12] have shown that as oxidation proceeds, average residual stress over the film decreases, with tentative increase at transition. Since monoclinic phase has larger specific volume than tetragonal phase, change into purely monoclinic phase is considered to be the result rather than the cause of oxide breakdown accompanying release of stress. Thus the high hydrogen absorption rate at transition and subsequent decreasing tendency could be qualitatively understood in terms of disturbance of the oxide film at transition. However, considerably different behaviors of Zr-Nb group and Zircaloys cannot be explained by the phase change alone. Godlewski et al. mentioned above have not reported any structural difference between Zr-1%Nb and Zircaloy-4.

General feature of the oxidation and hydriding behavior of Zr-Nb alloys in comparison to those of Zircaloys could be understood in terms of electrochemical properties of oxide film. The oxide films of the two kinds of alloys are essentially modified forms of zirconium oxide (ZrO_2), which are known to have two characters, one as ionic conductor and another as semiconductor. Its electrical conductivity is known to have a well-shaped dependency on O/M ratio: the bottom corresponds to the near-stoichiometry region and the two side walls having high conductivity corresponds to non-stoichiometry regions[13],[14]. The near-stoichiometry region shows the character as ionic conductor and serves practical purpose as oxygen meter.

Vest et al.[13] interpreted their measurements of electrical conductivity of monoclinic zirconia (ZrO_2) in terms of equilibrium between lattice defects and electronic charge carriers. In the sub-stoichimetric region, principal lattice defects are considered to be oxygen vacancies, whose concentration is determined by the following equilibrium:

$$V_O^{2+} + 1/2O_2 + 2e^- = O_{lattice} \qquad (1)$$

where V_O^{2+} is oxygen vacancy and e^- is electron in the conduction band. Considering that the concentration of lattice oxygen atoms is nearly constant, mass action law is written in the following form:

$$[V_O^{2+}]\ p(O_2)^{1/2}\ [e^-]^2 = K \tag{2}$$

where $p(O_2)$ is oxygen partial pressure (atm), K is equilibrium constant and parentheses represent concentrations.

Vest et al. assumed that in the highly sub-stoichiometric region, oxygen vacancies are mainly produced by reduction of zirconia and that the condition of electric neutrality must be locally satisfied:

$$[V_O^{2+}] = 2[e^-] \tag{3}$$

Then (2) is modified to give the dependency of the concentrations of oxygen vacancies and electrons on oxygen pressure as

$$[V_O^{2+}] = 2[e^-] \propto p(O_2)^{-1/6} \tag{4}$$

In the hyper-stoichiometric region, their measurements suggested the combination of zirconium vacancy and positive hole as major lattice defect and charge carrier, for which equilibrium equation is

$$V_{Zr}^{4-} + 2\ O_{lattice} + 4\ p^+ = O_2 \tag{5}$$

where V_{Zr}^{4-} and p^+ represent zirconium vacancy and positive hole, respectively.

In the region far from stoichiometry, condition of electric neutrality again simplifies the equation of mass action law to give oxygen pressure dependences of defect and electron concentrations as

$$[V_{Zr}^{4-}] = 4[p^+] \propto p_{O2}^{1/5} \tag{6}$$

These oxygen pressure exponents were found to fit their electrical conductivity data on the oxide of unalloyed zirconium. Even if other type combinations of lattice defect and charge carrier were assumed, only slight changes are necessary for these exponents. The important point is that defect concentration depends on oxygen pressure as

$p_{O2}^{-1/m}$ in the far substoichiometric region and as $p_{O2}^{1/m}$ in the far hyper-stoichiometric region where m is an integer of 3 to 6.

Then assuming the same combinations of lattice defect and charge carrier, we shall examine the effect of alloying elements on those pressure exponents. Major valency of niobium is 5 corresponding to Nb_2O_5. From the analogy to the impurity effect in silicon, niobium atoms incorporated into ZrO_2 lattice will work as electron donor, enhancing the character as n-type semiconductor. In the hypo-stoichiometric region, equation of mass action law (2) still holds, but the condition of neutrality (3) no longer holds. In the extreme case, if we assume that concentration of electrons is essentially determined by the contribution from niobium, it drops from (2) as a constant and oxygen vacancy concentration will depend on oxygen pressure as

$$[V_O^{2+}] = C\ p_{O2}^{-1/2} \tag{7}$$

On the other hand, major alloying element of Zircaloys, tin, has a principal valency of 3. Tin atoms incorporated into the zirconia lattice will therefore supply positive holes. Then the condition of neutrality requires the following relationship:

$$2[V_O^{2+}] + [p^+] = [Sn^-] + [e^-] \tag{8}$$

If we assume that the concentration of tin ion is significantly high but the positive holes are annihilated by combination with electrons, we get

$$2[V_O^{2+}] = [Sn^-] + [e^-] \tag{9}$$

where

$$[e^-] \ll [Sn^-] \tag{10}$$

It means that oxygen vacancy concentration is nearly independent of oxygen partial pressure, and equation (2) gives oxygen pressure dependency of electron concentration as

$$[e^-] = \text{const.}\ p_{O2}^{-1/4} \tag{11}$$

The actual situation will of cource be much more complex.

Basically, however, in the hypo-stoichiometric region addition of niobium to zirconia will make the oxygen pressure dependency of defect concentration greater (steeper slope of 'side wall'), whereas addition of tin (Zircaloys) will makes the dependency smaller. In the hyper-stoichiometric region, the opposite effects of alloying elements are deduced.

The concnetration of lattice defects concerns primarily diffusion rate of oxygen (oxidation). However, the present kinetic data and many corrosion data on zirconium alloys imply close relationship between oxidation and hydriding rates. If we assume the same type of dependency of oxygen transport and hydrogen transport on lattice defect concentration, then the above-discussed dependency on oxygen pressure could explain the general feature of the present results.

Hydriding of pre-oxidized specimens in the present oxperiment was performed by closing purified hydrogen gas with specimens. It means that the atmosphere was strongly reducing but that oxygen partial pressure (explicitly, realized by H_2O/H_2 ratio) was left uncontrolled. Then, in Zr-Nb alloys, run-to-run difference of oxygen potential will have resulted in large difference in hydriding rate because of the strong (negative in sign) dependency of defect concentration on oxygen pressure. In Zircaloys, on the other hand, the effect of uncontrolled atmosphere would have been much smaller because of the smaller (in absolute value) oxygen pressure exponents of defect concentration in the hypostoichiometric region. It can qualitatively explain, at least in the post-transition region, why such a large run-to-run difference was observed in Zr-Nb alloys and why the behavior of Zircaloys was rather stable.

The above basic understanding can explain several other findings of the present experiment, though many other detailed points remain unexplained, as follows:

1) It can explain why Zircaloys were superior (smaller in rate) to Zr-Nb alloys in (pre-transition) oxidation resistance and why Zr-Nbs were generally superior to Zircaloys in resistance against hydriding. The above equilibrium consideration concerns primarily oxygen pressure dependencies of defect concentrations. However, addition of niobium and tin to zirconia will work, not only to change the gradient, but also to reduce the absolute defect concentrations in the hypo-stoichiometric and hyper-stoichiometric regions, respec-

tively. Thus the two groups of alloy will have smaller transport properties in the two respective regions. A natural consequence of this discussion is that better corrosion resistance of Zr-Nb relative to Zircaloy will be exhibited in more reducing atmosphere. It is supported, as long as out-pile corrosion rate is concerned, by a comparative test result[15].

2) It can explain why rather large difference was observed between the hydriding behaviors of Zr-1%Nb and that of Zr-2.5%Nb, whereas the difference between Zircaloy-2 and Zircaloy-4 was negligible. In the metal phase, solubility of Nb in Zr is 0.6 % at 620°C[16]. Zr-1%Nb and -2.5%Nb are therefore both precipitation type alloys. As oxide, the solubility of Nb_2O_5 in ZrO_2 is about 9 %[17]. The oxides of the two Zr-Nb alloys are therefore both in the solid solution side. It is difficult to explain the difference between the two Zr-Nb alloys only by phase relationship. When the electronic effect of Nb addition into ZrO_2 lattice is considered, the difference between 1 % and 2.5 % will become more significant.

Considering that the electronic effect of Nb addition is dominant in the highly hypo-stoichiometric region, it is understandable that the difference of the two alloys was evident in the hydriding step, not in the oxidation step. Also it is no wonder that the diference of the oxide property which caused different hydriding behaviors could not be detected by means of X-ray diffraction nor by metallography.

3) The data on the partition of hydrogen between the metal and the oxide (Table 2) become easier to understand, at least qualitatively, by considering the electronic effect of alloying elements. The Table 2 data on Zr-Nb show a general feature that when the hydrogen absorption across the oxide film is rapid, the part of hydrogen remaining in the oxide is also large. This feature denies the possibility that hydrogen is transported via some short-circuting paths. It implies that when the hydrogen permeabilty of the oxide is large, it is a result of some bulk property change of the oxide.

The hydrogen partition behavior of Zircaloys seems a little different from that of Zr-Nbs, though the small number of data prevents definate conclusion. Roy[18] studied the partition of tritium between the metal and the oxide of unalloyed zirconium by autoradiography. He found that in specimens with thick oxide,

tritium existed mainly in the metal side and the tritium remaining in the oxide was segregated along numerous thin lines, probably showing micro-cracks. The distribution of hydrogen (tritium) he observed in zirconium seems to fit the behavior of Zircaloys in the present experiment.

From the above discussions, a conclusion is produced that out of the hydrogen absorption data for Zr-Nb (particularly Zr-2.5%Nb) having large scatter, the data forming the lower limit have practical importance. It is because the transport path for exygen and hydrogen during actual corrosion must consist of different O/M regions in series and the region with the smallest transport property will be rate-determining. Under the uncontroled oxygen activity in the present experiment, data points showing considerable absorption rate beside the points showing null absorption will have to be regarded merely as results of too low O/M ratio of the entire oxide film. In this meaning, the observation of low hydrogen absorption rate in the Zr-2.5%Nb oxidized deeply into the post-transition region is a fact in favor of using the alloy as high-burnup fuel cladding.

5. conclusion

Zr-Nb and Zircaloy tube specimens were heated in hydrogen gas after accelerated oxidation to post-transition region in steam, oxygen and air and hydrogen absorption ratio was measured. The following tendencies were observed:

1) Hydrogen absorption ratio by Zircaloy was relatively insensitive to the kind of oxidant used for pre-oxidation, whereas that of Zr-Nb was dependent on the pre-oxidation condition, oxidation in oxygen resulting in the poorest resistance to hydrogen absorption.
2) Transition in oxidation kinetics was found to result in high absorption rate in subsequent hydriding in all materials. When pre-oxidation was made deep into the post-transition region in steam or air, absorption rate by Zr-Nb, particularly by Zr-2.5%Nb, was found to decrease with oxidation level. On the other hand, the absorption rate by Zircaloy was nearly constant in the same region.
3) Evidences were derived which suggest that absorption property of the Zr-Nb alloys is determined by the bulk transport property of the oxide film rather than presence or absence of short-circuiting paths.

tritium existed mainly in the metal side and the tritium remaining in the oxide was segregated along numerous thin lines, probably showing micro-cracks. The distribution of hydrogen (tritium) he observed in zirconium seems to fit the behavior of Zircaloys in the present experiment.

From the above discussions, a conclusion is produced that out of the hydrogen absorption data for Zr-Nb (particularly Zr-2.5%Nb) having large scatter, the data forming the lower limit have practical importance. It is because the transport path for exygen and hydrogen during actual corrosion must consist of different O/M regions in series and the region with the smallest transport property will be rate-determining. Under the uncontroled oxygen activity in the present experiment, data points showing considerable absorption rate beside the points showing null absorption will have to be regarded merely as results of too low O/M ratio of the entire oxide film. In this meaning, the observation of low hydrogen absorption rate in the Zr-2.5%Nb oxidized deeply into the post-transition region is a fact in favor of using the alloy as high-burnup fuel cladding.

5. conclusion

Zr-Nb and Zircaloy tube specimens were heated in hydrogen gas after accelerated oxidation to post-transition region in steam, oxygen and air and hydrogen absorption ratio was measured. The following tendencies were observed:

1) Hydrogen absorption ratio by Zircaloy was relatively insensitive to the kind of oxidant used for pre-oxidation, whereas that of Zr-Nb was dependent on the pre-oxidation condition, oxidation in oxygen resulting in the poorest resistance to hydrogen absorption.
2) Transition in oxidation kinetics was found to result in high absorption rate in subsequent hydriding in all materials. When pre-oxidation was made deep into the post-transition region in steam or air, absorption rate by Zr-Nb, particularly by Zr-2.5%Nb, was found to decrease with oxidation level. On the other hand, the absorption rate by Zircaloy was nearly constant in the same region.
3) Evidences were derived which suggest that absorption property of the Zr-Nb alloys is determined by the bulk transport property of the oxide film rather than presence or absence of short-circuiting paths.

Acknowledgement

The author acknowledges the useful discussions on the test results with Dr. S. Kawasaki and Mr. T. Furuta. He is also grateful to Mr. S. Iso for the gas chromatography analysis of hydrogen and to Dr. N. Masaki for his assistance in X-ray diffraction analysis.

References

1) Kiselev, A.A. et al., "Research on the corrosion of zirconium alloys in water and steam at high temperature and pressure", Corrosion of Reactor Materials, Proceedings of the IAEA Conference at Saltzburg 4-8 June, 1962, II p.67
2) Hillner, E., "Corrosion of zirconium-base alloys-an overview", Zirconium in the Nuclear Industry, ASTM STP 633 (1976) p.211
3) Hardy, D.G., Wood, J.C., and Urbanic, V.F., "Zirconium-niobium alloys as fuel cladding for water cooled reactors", Fabrication of Water Reactor Fuel Element, Proceeding Series IAEA-SM-233/32 (1979) p.463
4) Dalgaard, S.B., "Corrosion and hydriding behaviour of some Zr-2.5 w/o Nb alloys in water steam and various gases at high temperature", Corrosion of Reactor Materials, Proceedings of the IAEA Conferenc at Saltzburg 4-8 June 1962, II p.159
5) Boulton, J., "The corrosion of zirconium alloys", ibid., p.133
6) Cox, B., Chadd, P.G., and Short, J.F., "The oxidation and corrosion of zirconium and its alloys. XV, further studies of zirconium-niobium alloys", AERE R 4134 (1962)
7) Von Rubel, H., Debray, W., and Roesler, U., "Wasserstoffaufnahme und Wasserstoffversproedung von Zircaloy-2, ZrNb 1 und ZrNb 2.5", Nukleokik 6 (1964) 13
8) Aronson, S., "Some experiments on the permeation of hydrogen through oxide films on zirconium", WAPD-BT-19 (1960)
9) Shannon, D.W., "Role of the oxidation rate on the hydriding of zirconium alloys in gas atmospheres containing hydrogen", HW-76562 (1963)
10) Boyle, R.F. and Kisiel, T.J., "Hydrogen permeation of Zircaloy-2 Corrosion films", WAPD-BT-10 (1958)
11) Godlewski, J. et al., "Raman spectroscopy of the tetragonal to

Acknowledgement

The author acknowledges the useful discussions on the test results with Dr. S. Kawasaki and Mr. T. Furuta. He is also grateful to Mr. S. Iso for the gas chromatography analysis of hydrogen and to Dr. N. Masaki for his assistance in X-ray diffraction analysis.

References

1) Kiselev, A.A. et al., "Research on the corrosion of zirconium alloys in water and steam at high temperature and pressure", Corrosion of Reactor Materials, Proceedings of the IAEA Conference at Saltzburg 4-8 June, 1962, II p.67
2) Hillner, E., "Corrosion of zirconium-base alloys-an overview", Zirconium in the Nuclear Industry, ASTM STP 633 (1976) p.211
3) Hardy, D.G., Wood, J.C., and Urbanic, V.F., "Zirconium-niobium alloys as fuel cladding for water cooled reactors", Fabrication of Water Reactor Fuel Element, Proceeding Series IAEA-SM-233/32 (1979) p.463
4) Dalgaard, S.B., "Corrosion and hydriding behaviour of some Zr-2.5 w/o Nb alloys in water steam and various gases at high temperature", Corrosion of Reactor Materials, Proceedings of the IAEA Conferenc at Saltzburg 4-8 June 1962, II p.159
5) Boulton, J., "The corrosion of zirconium alloys", ibid., p.133
6) Cox, B., Chadd, P.G., and Short, J.F., "The oxidation and corrosion of zirconium and its alloys. XV, further studies of zirconium-niobium alloys", AERE R 4134 (1962)
7) Von Rubel, H., Debray, W., and Roesler, U., "Wasserstoffaufnahme und Wasserstoffversproedung von Zircaloy-2, ZrNb 1 und ZrNb 2.5", Nukleokik 6 (1964) 13
8) Aronson, S., "Some experiments on the permeation of hydrogen through oxide films on zirconium", WAPD-BT-19 (1960)
9) Shannon, D.W., "Role of the oxidation rate on the hydriding of zirconium alloys in gas atmospheres containing hydrogen", HW-76562 (1963)
10) Boyle, R.F. and Kisiel, T.J., "Hydrogen permeation of Zircaloy-2 Corrosion films", WAPD-BT-10 (1958)
11) Godlewski, J. et al., "Raman spectroscopy of the tetragonal to

monoclinic transition in zirconium oxide scales and determination of overall oxygen diffusion by nuclear microanalysis of O^{18}", Paper presented at 9th IAEA Meeting on Zirconium in Nuclear Industry, Nov. 5-8, 1990, Kobe Japan

12) Garzarolli, F. et al., "Oxide growth mechanism on zirconium alloys", ibid.

13) Vest, R.M., Tallan, N.M., and Tripp, W.C., "Electrical properties and defect of zirconia, I. monoclinic phase", J. Amer. Ceram. Soc. 47(1964) p.635

14) Kofstad, P. and Ruzicka, D.J., "On the defect structure of ZrO_2 and HfO_2", J. Electrochem. Soc. 110(1963) p.181

15) LeSurf, J.E. and Bryant, P.E.C., "The effect of water chemistry on the oxidation of zirconium alloys under reactor radiation", AECL-2797 (1968)

16) Massalski, T.B., "Binary alloy phase diagrams", Am. Soc. Met. (1986)

17) Rinehart, G.H., "High temperature thermodynamics and vaporization of the zirconium-niobium-oxygen system", COO-1140-224 (1978)

18) Roy, C., "Hydrogen distribution in oxidized zirconium alloys by autoradiography", AECL-2085 (1964)

Table 1 Properties of tube specimens

	Zr-1%Nb	Zr-2.5%Nb	Zry-2	Zry-4
outer dia. (mm)	16.46	13.48	12.23	10.72
wall thickness (mm)	0.80	0.41	0.70	0.62
heat treatment	480°C	485°C 2 hr	500°C 4 hr	
oxygen content(ppm)	1060	1180	1300	1250
hydrogen (ppm)	23	< 5	< 5	16
R.T. 0.2%YS (MPa)	471	545	539	610
UTS (MPa)	632	710	673	778
elong. (%)	28	25	20	17

Table 2 Results of chemical analysis for hydrogen content

No.	material	oxidation		hydriding	hydrogen content (ppm)	
		atmos.	w. gain (mg/dm^2)	(*1) (ppm)	with oxide	without oxide
N1-76	Zr-1%Nb	steam	90	920	1070	730
N1-85	Zr-1%Nb	oxygen	462	1150	1440	730
N1-103	Zr-1%Nb	steam	520	134	840	770
N5-81	Zr-2.5%Nb	steam	217	341	550	520
N5-X-11	Zr-2.5%Nb	oxygen	357	442	610	510
N5-102	Zr-2.5%Nb	steam	425	70	750	800
N5-103	Zr-2.5%Nb	steam	465	0	690	910
Y4-72	Zry-4	steam	405	316	1620	1820
Y4-82	Zry-4	oxygen	314	258	380	330

*1 excludes hydrogen pickup during oxidation.

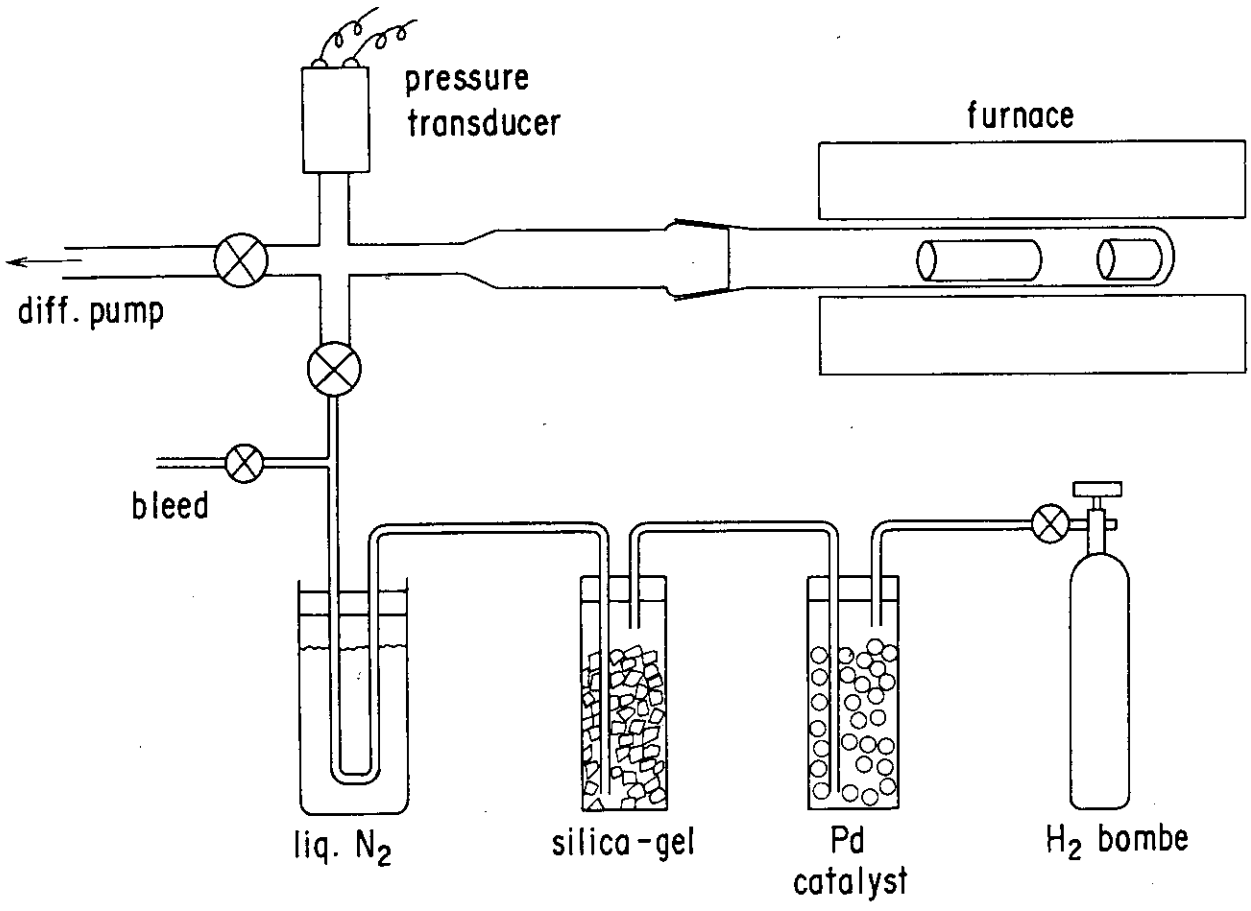

Fig. 1 Hydriding apparatus

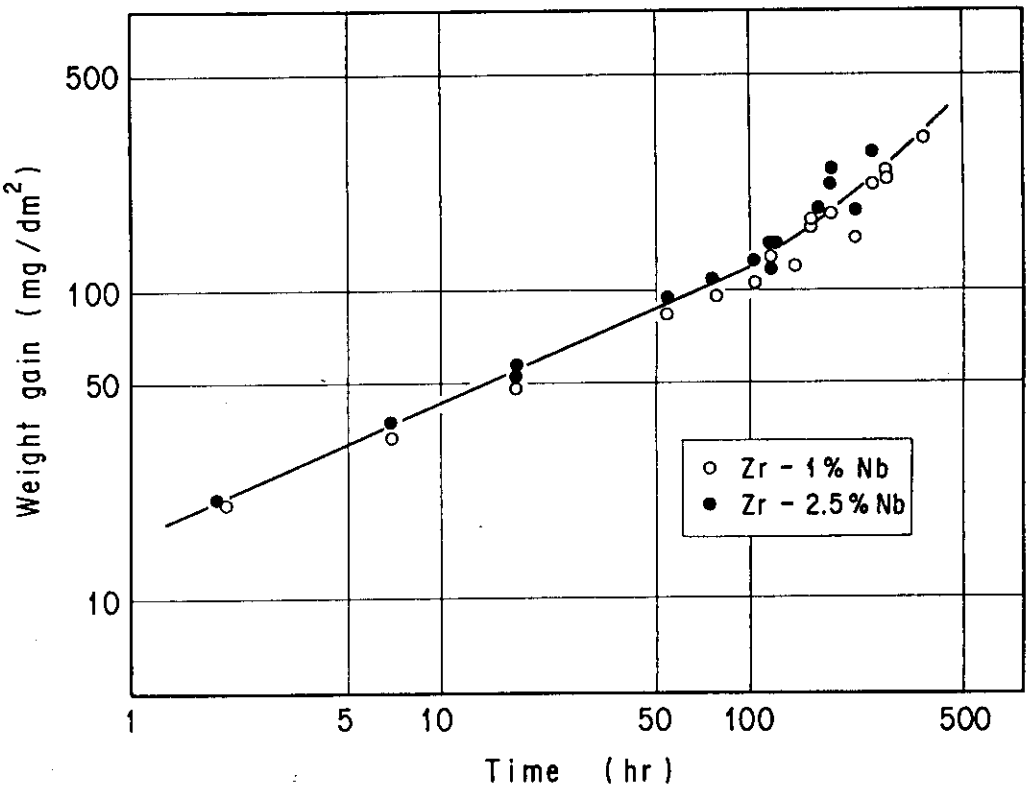

(a) Zr-Nb

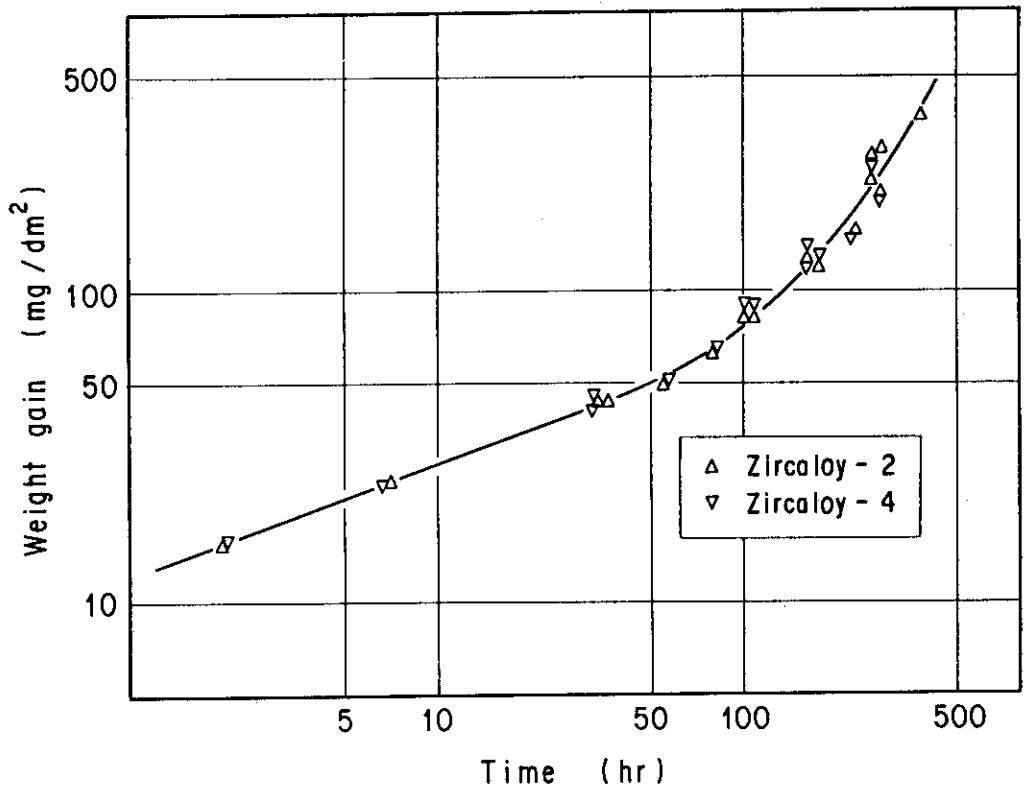

(b) Zircaloys

Fig. 2 Kinetics of oxidation in air at 500°C

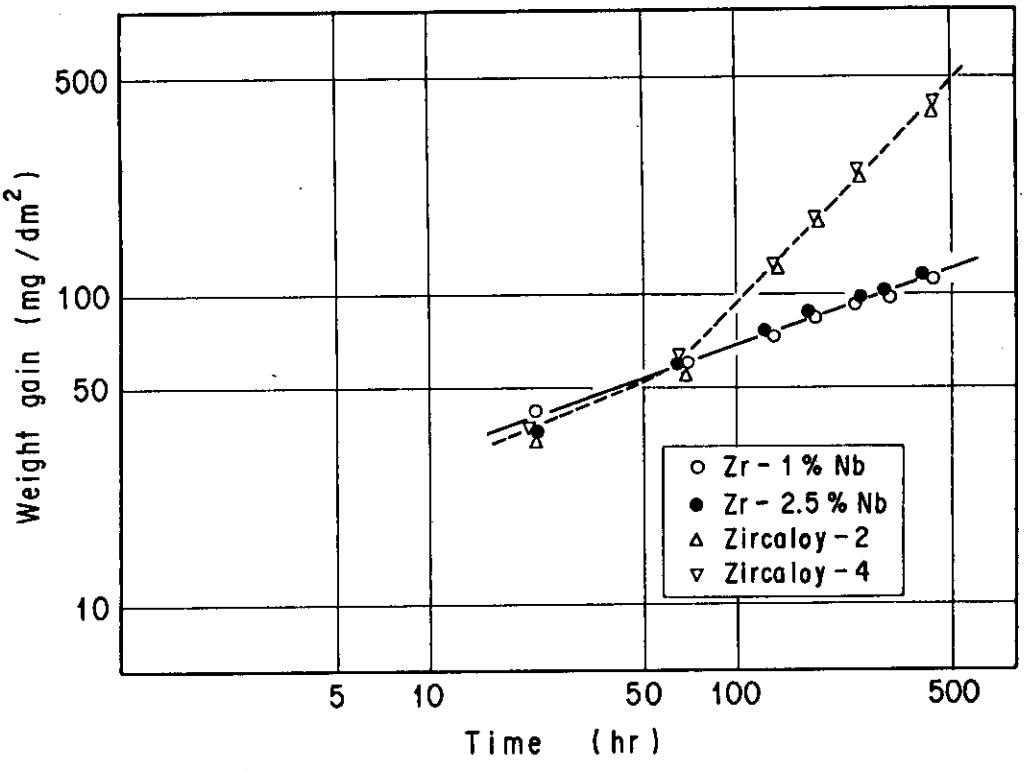

(a) 500°C

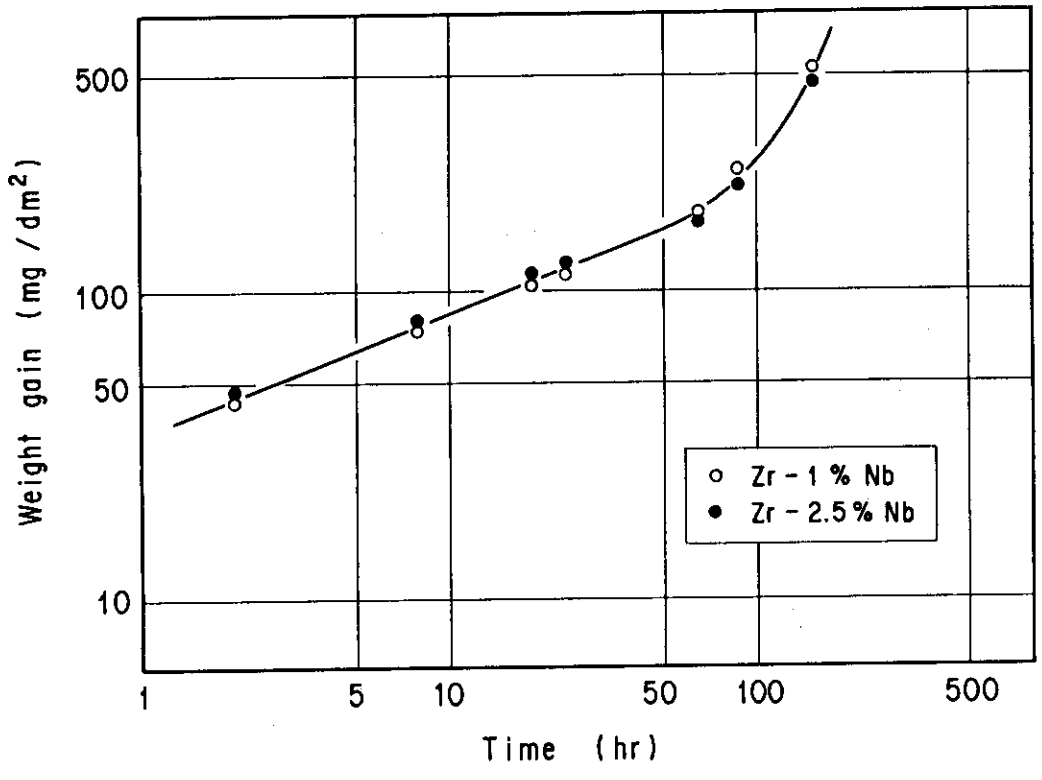

(b) 600°C

Fig. 3 Kinetics of oxidation in steam

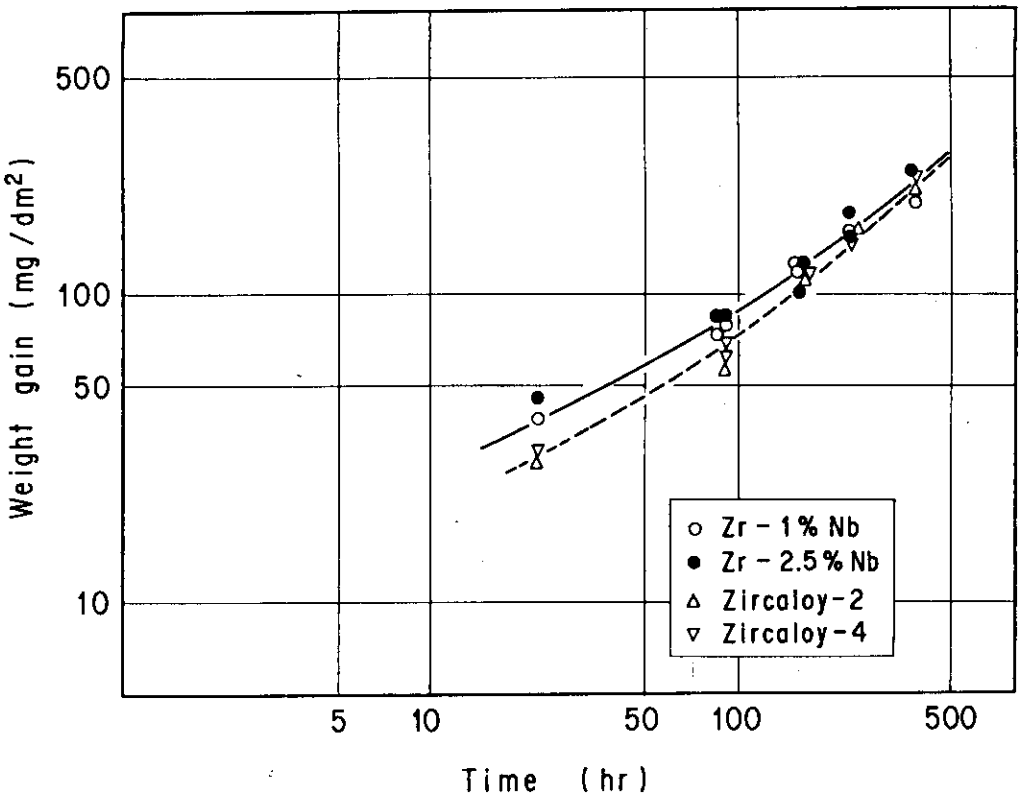

(a) 500°C

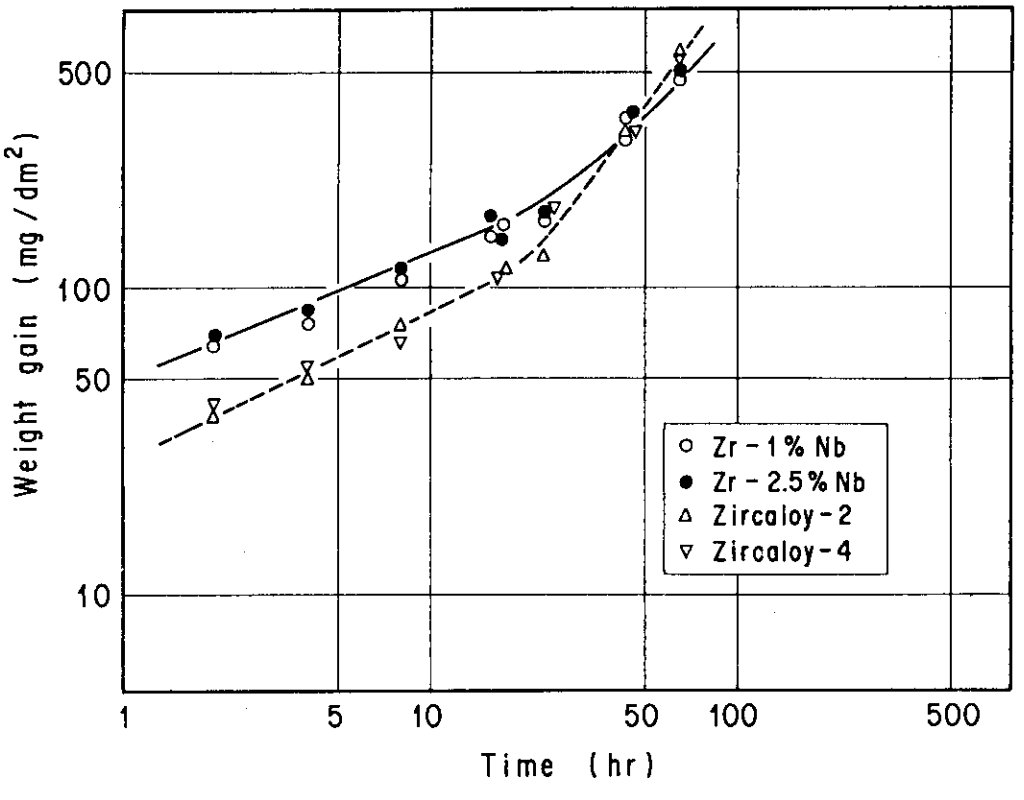

(b) 600°C

Fig. 4 Kinetics of oxidation in oxygen

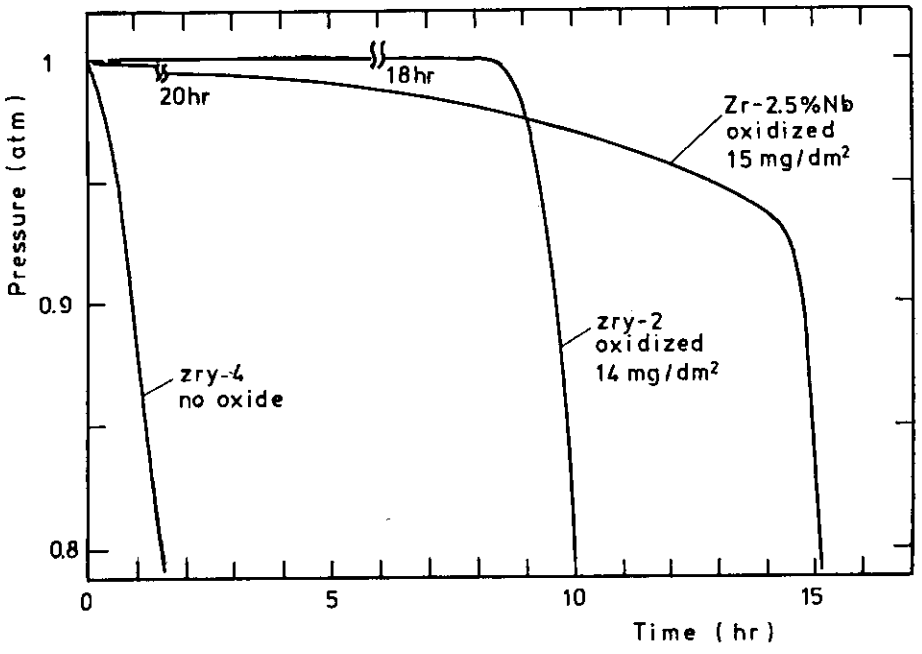

Fig. 5 Examples of pressure decrease due to hydrogen absorption

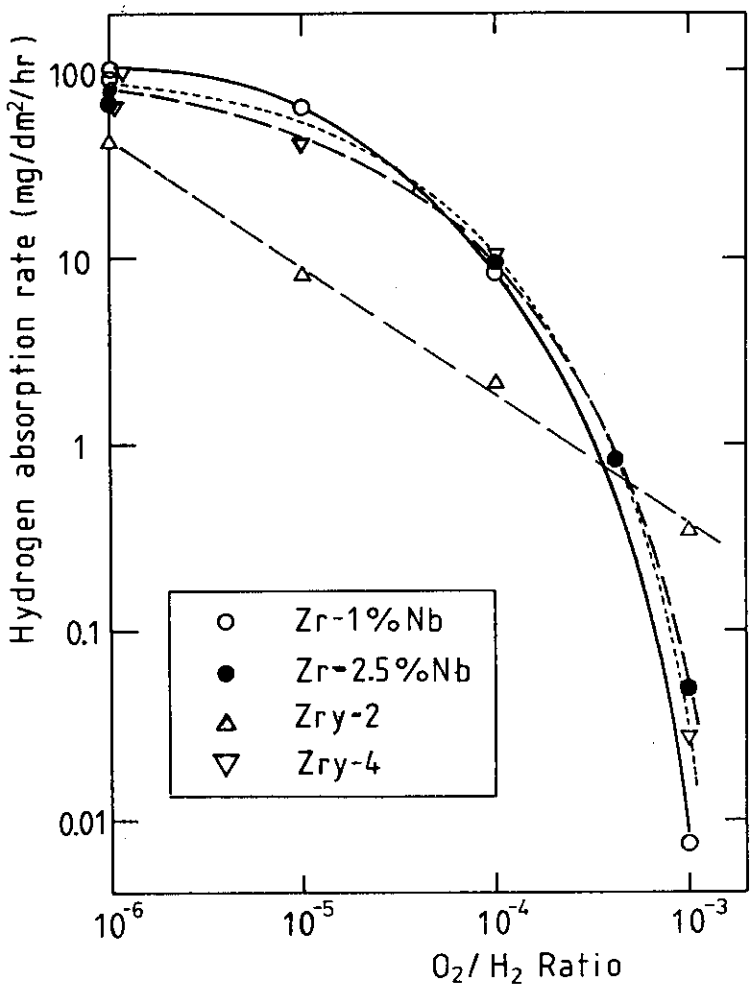

Fig. 6 Hydrogen absorption rates by unoxidized specimens

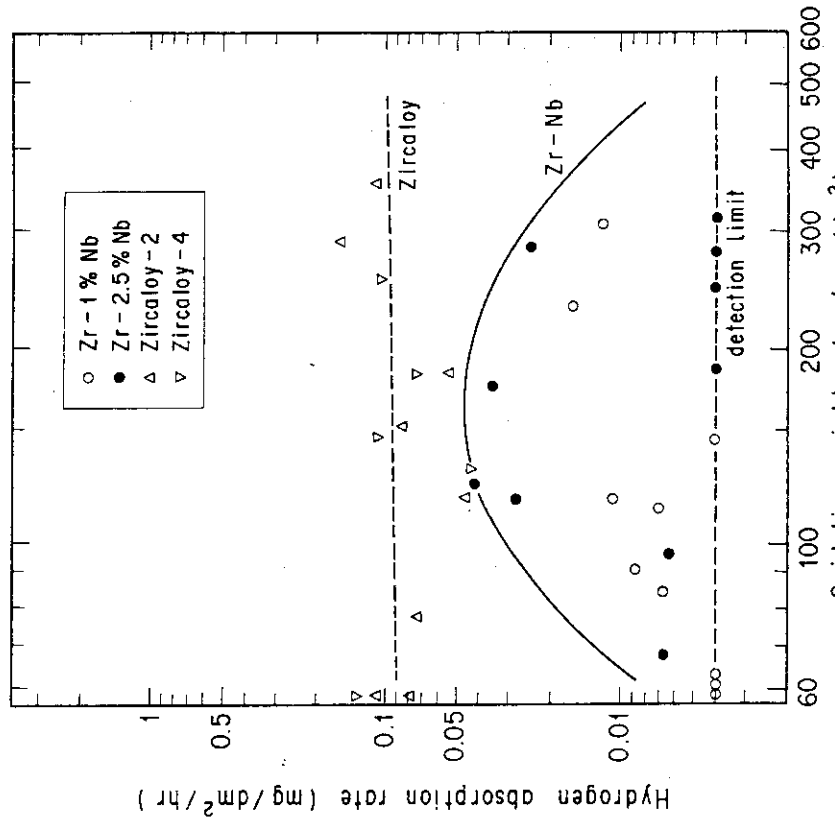

Fig. 8 Hydrogen absorption rates against oxidation level in air-oxidized specimens

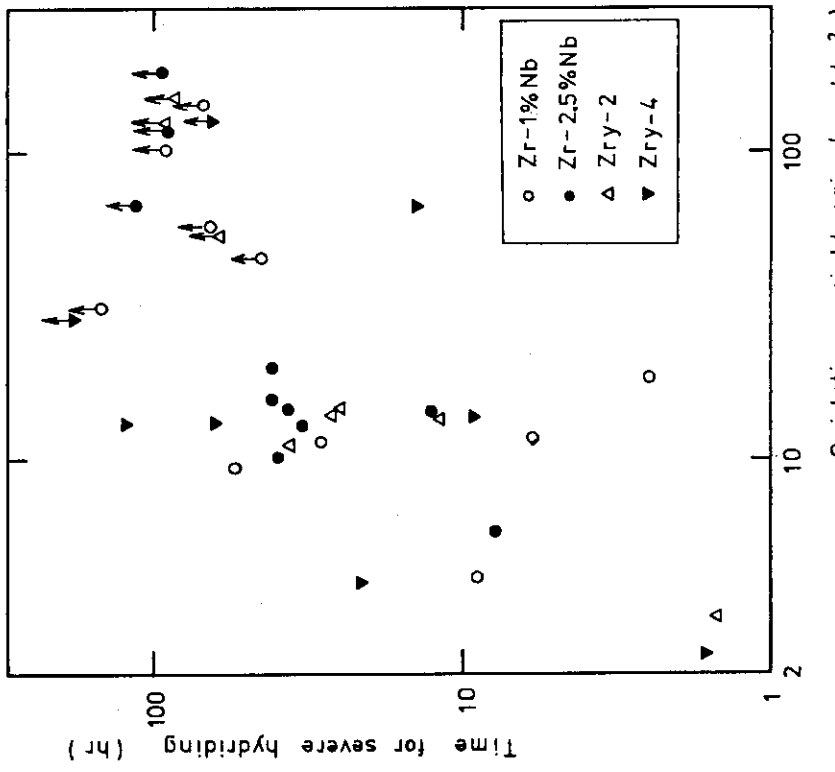

Fig. 7 Heating time before occurence of catastrophic hydriding against (air) pre-oxidation level (Upward arrows mean that catastrophic absorption did not occur within the time indicated.)

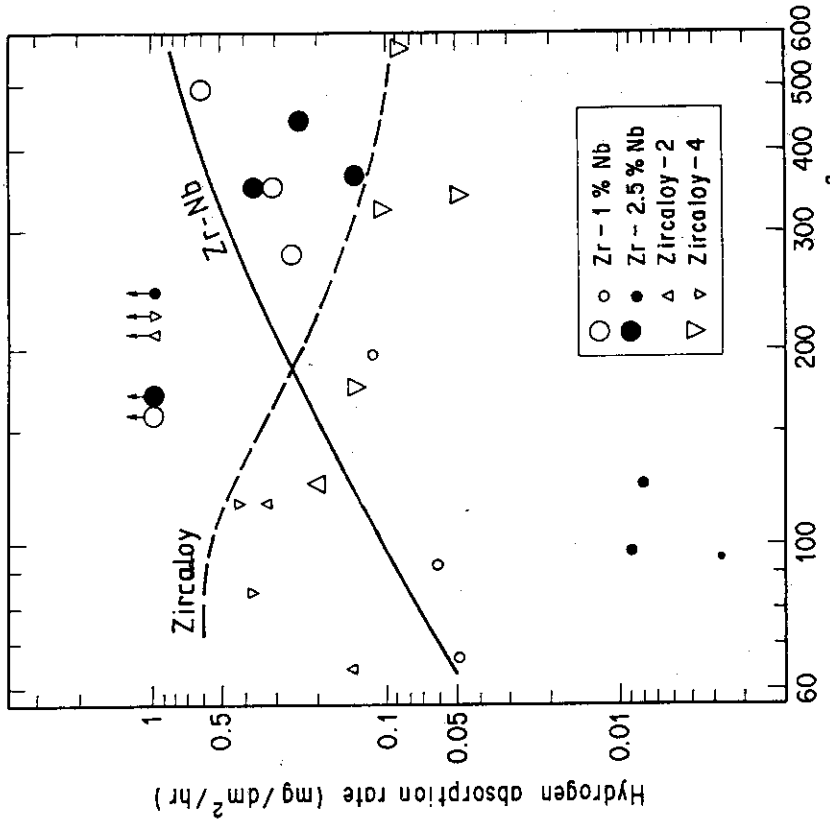

Fig. 10 Hydrogen absorption rates against oxidation level in specimens oxidized in oxygen (Small and large symbols represent the samples oxidized at 500°C and 600°C, respectively. Symboles with upward arrows mean that the run with the respective samples ended with catastrophic absorption.)

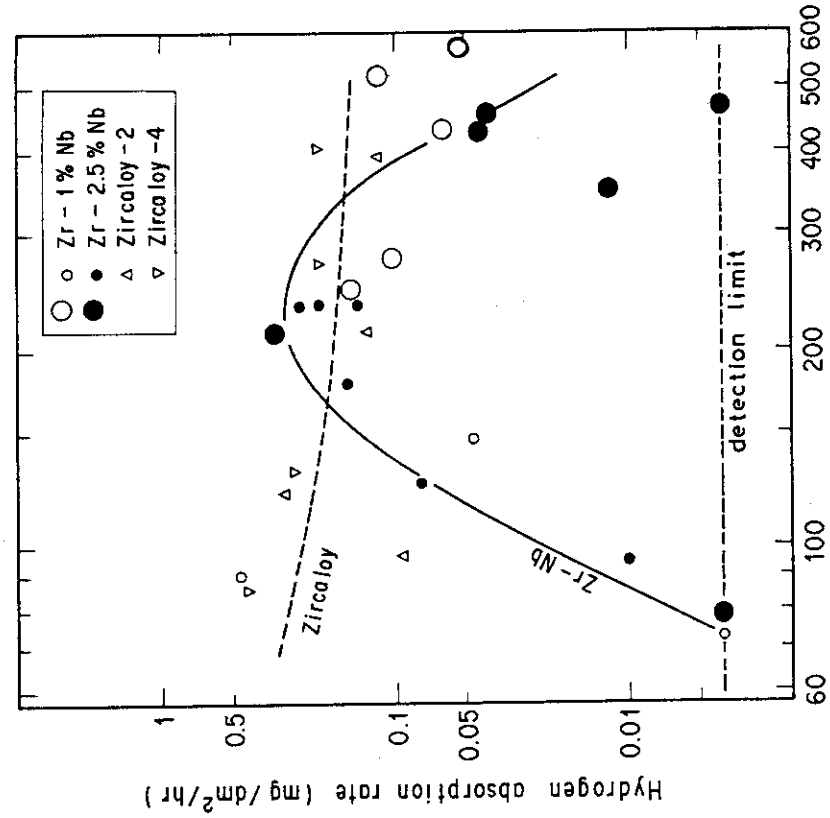

Fig. 9 Hydrogen absorption rates against oxidation level in steam-oxidized specimens (Small and large symboles represent the samples oxidized at 500°C and 600°C, respectively.)

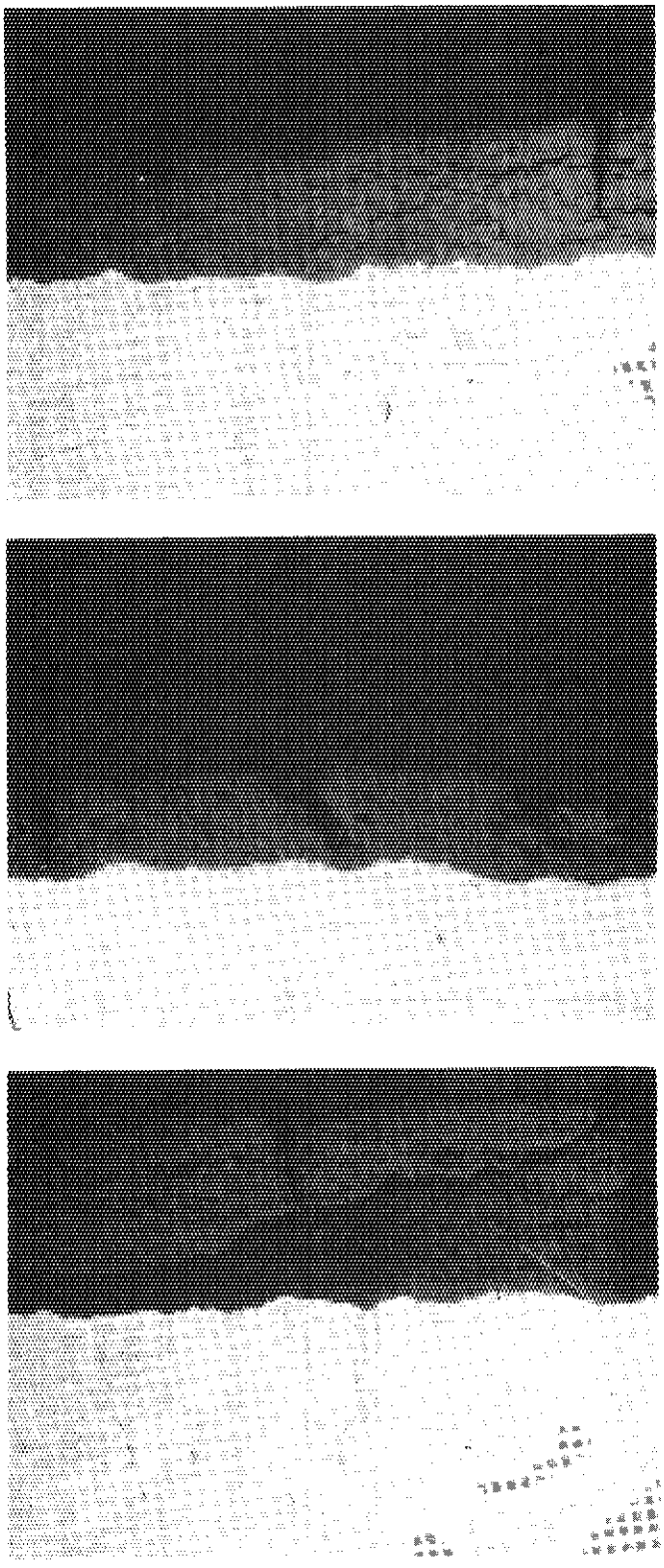

(a) Zr-1%Nb
oxidized
520 mg/dm^2
hydrided 134 ppm

(b) Zr-2.5%Nb
oxidized
465 mg/dm^2
no hydrogen
absorption

(c) zircaloy-4
oxidized
662 mg/dm^2
hydrided 108 ppm

Fig. 11 Oxide films grown in steam (x 400, outside surface)

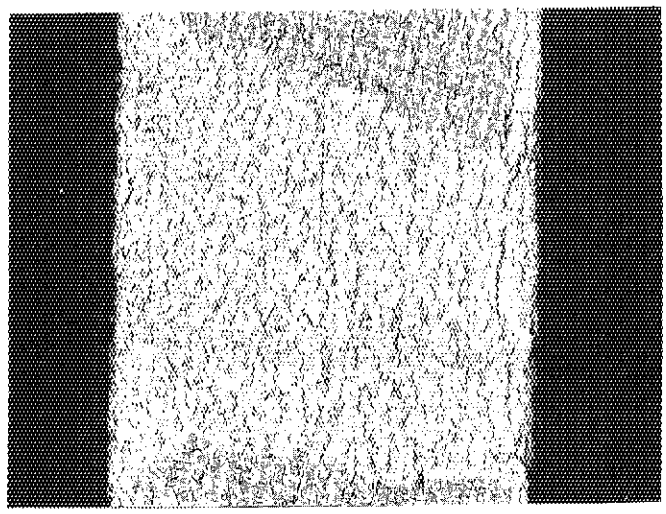

(a) Zr-1%Nb
oxidized (oxygen)
485 mg/dm^2
hydrided 465 ppm

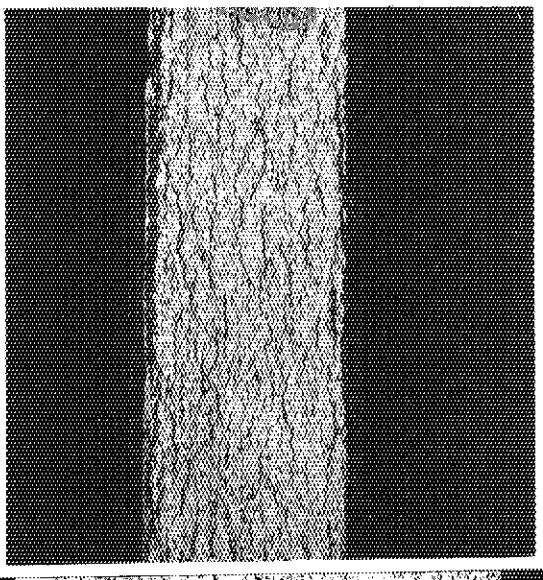

(b) Zr-2.5%Nb
oxidized (oxygen)
318 mg/dm^2
hydrided 150 ppm

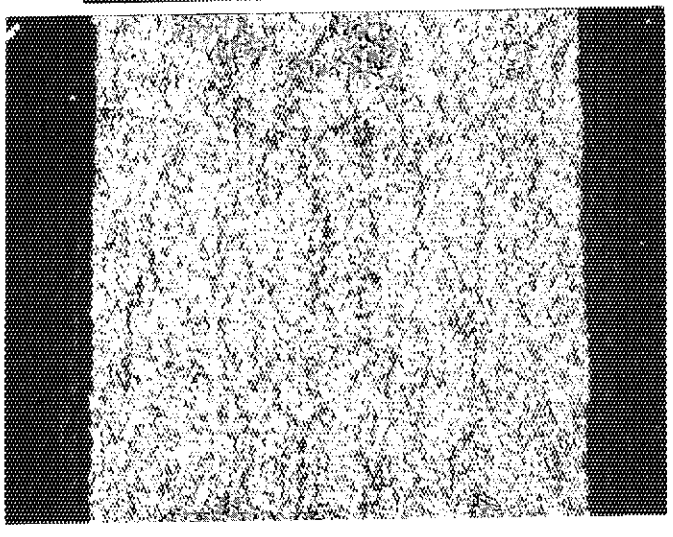

(c) Zircaloy-4
oxidized (oxygen)
571 mg/dm^2
hydrided 65 ppm

Fig. 12 Hydride precipitates after hydrogen absorption
(x 100 Left side is outer surface.)

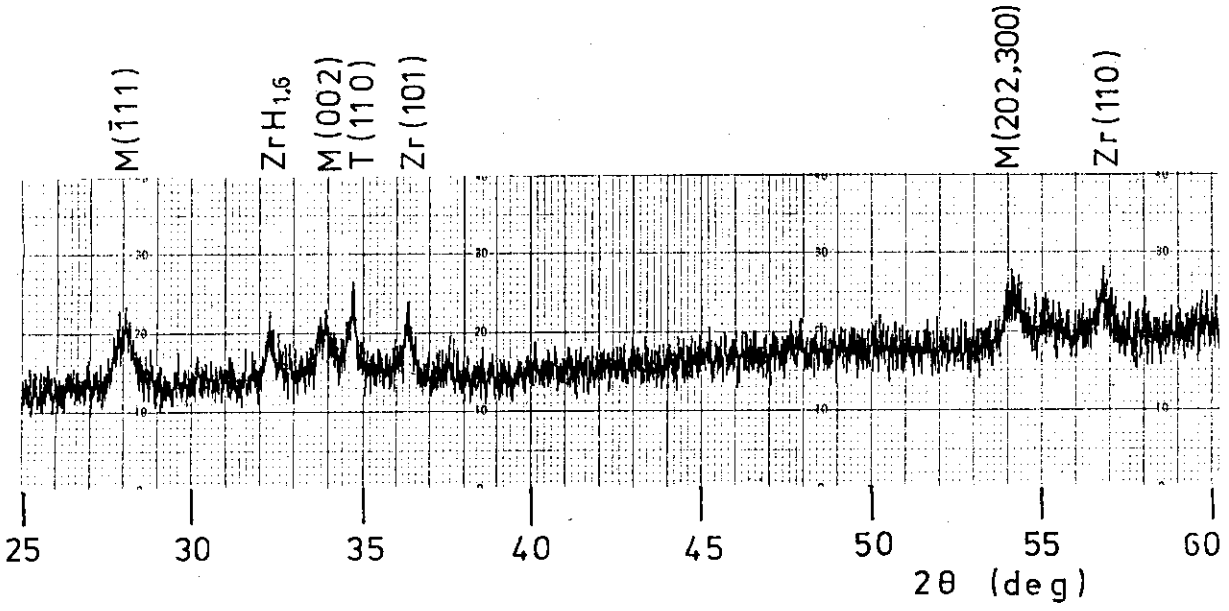

(a) Zr-1%Nb oxidized in air to 18 mg/dm^2

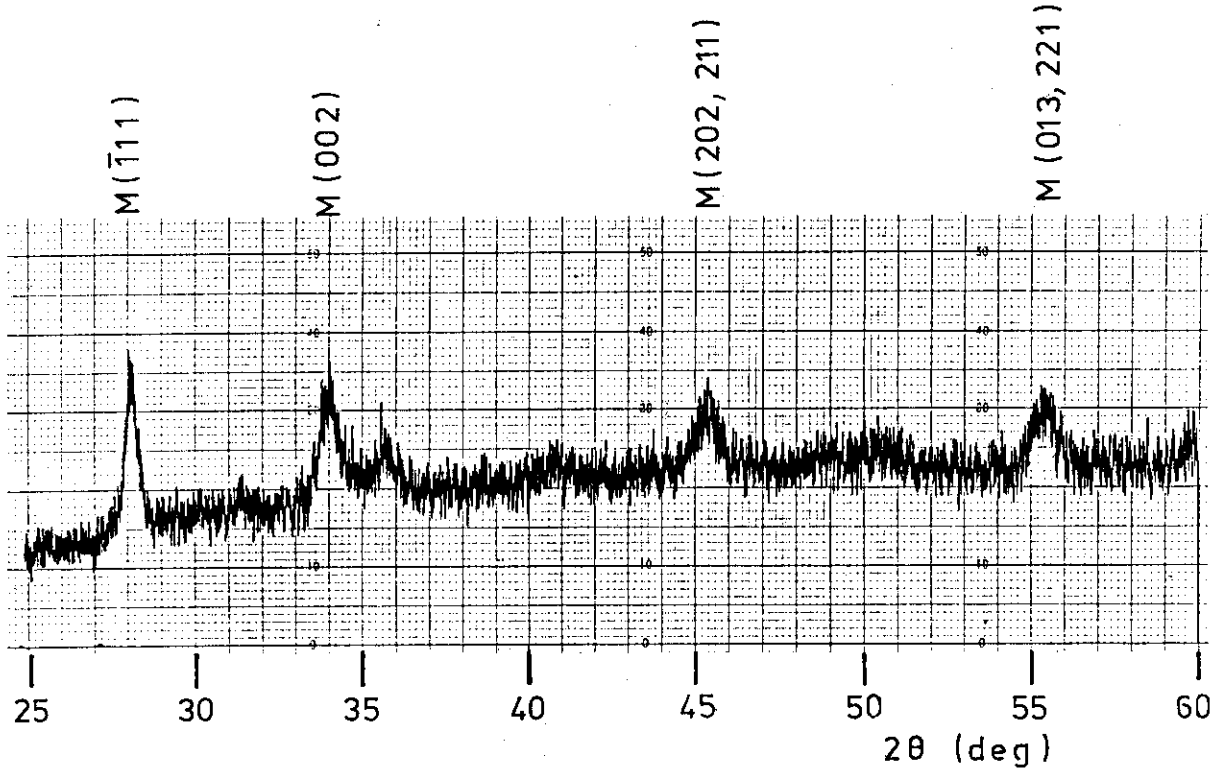

(b) Zr-2.5%Nb oxidized in oxygen to 446 mg/dm^2 and hydrided to 318 ppm.

Fig. 13 X-ray diffraction pattern by oxide films (Indices M and T mean monoclinic and tetragonal zirconia, respectively.)

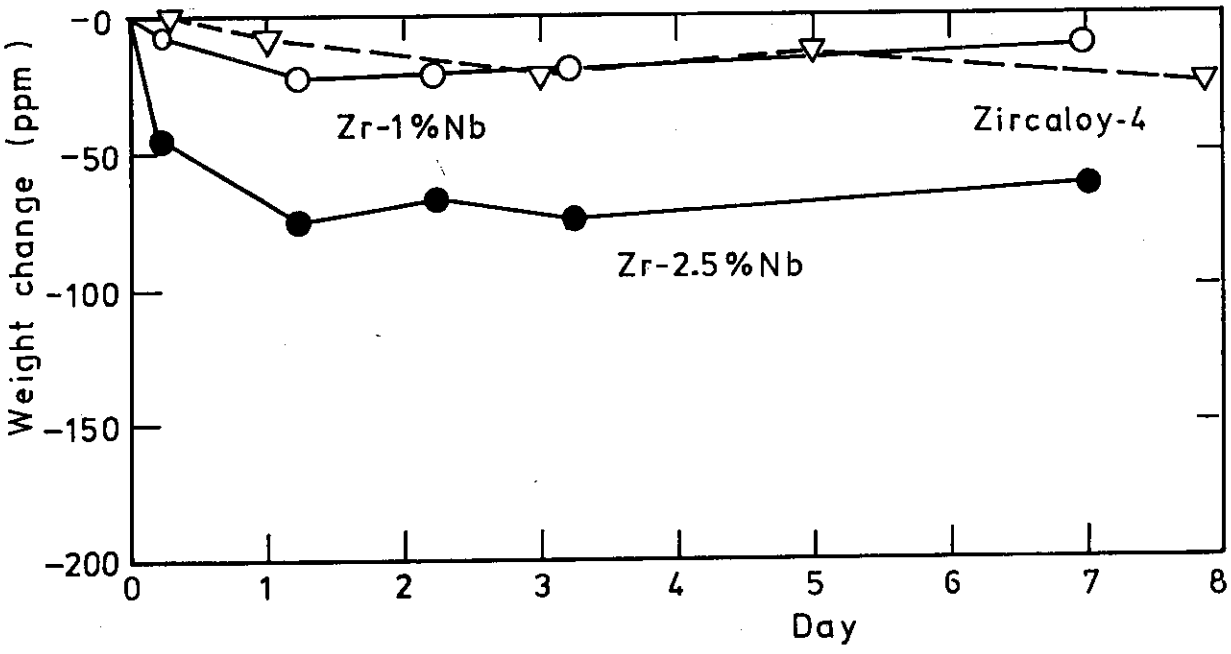

(a) pre-oxidized in steam and then hydrided

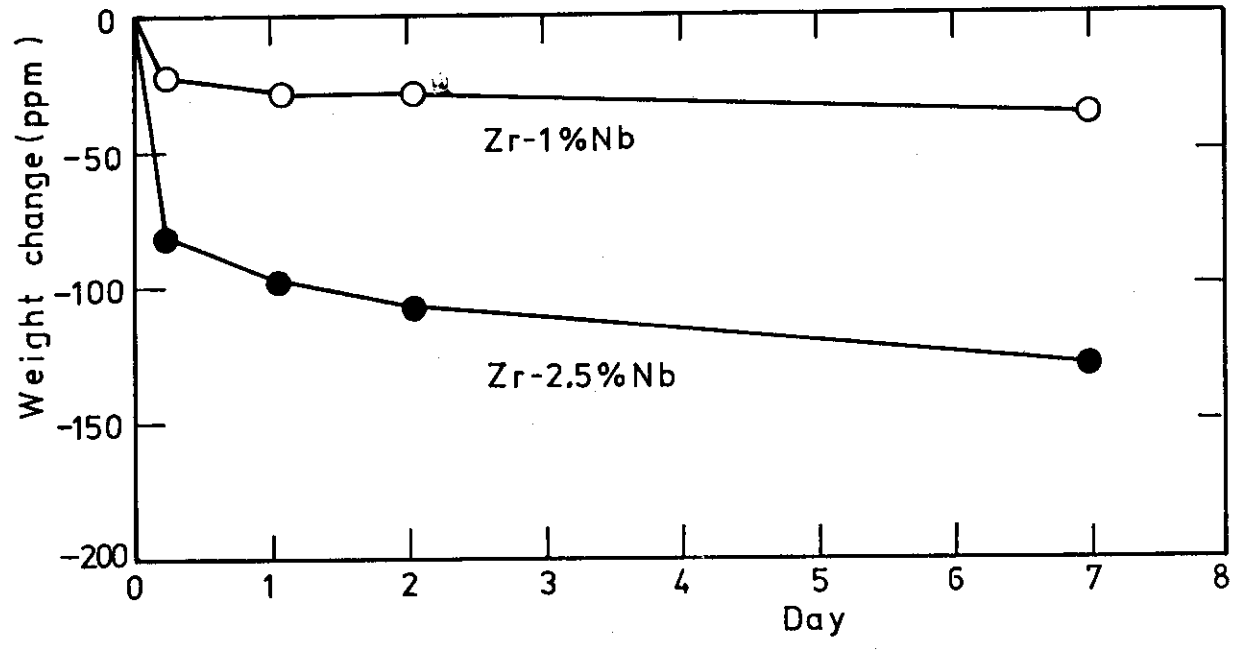

(b) pre-oxidized in oxygen and then hydrided

Fig. 14 Weight reduction at room temperature after hydrogen absorption

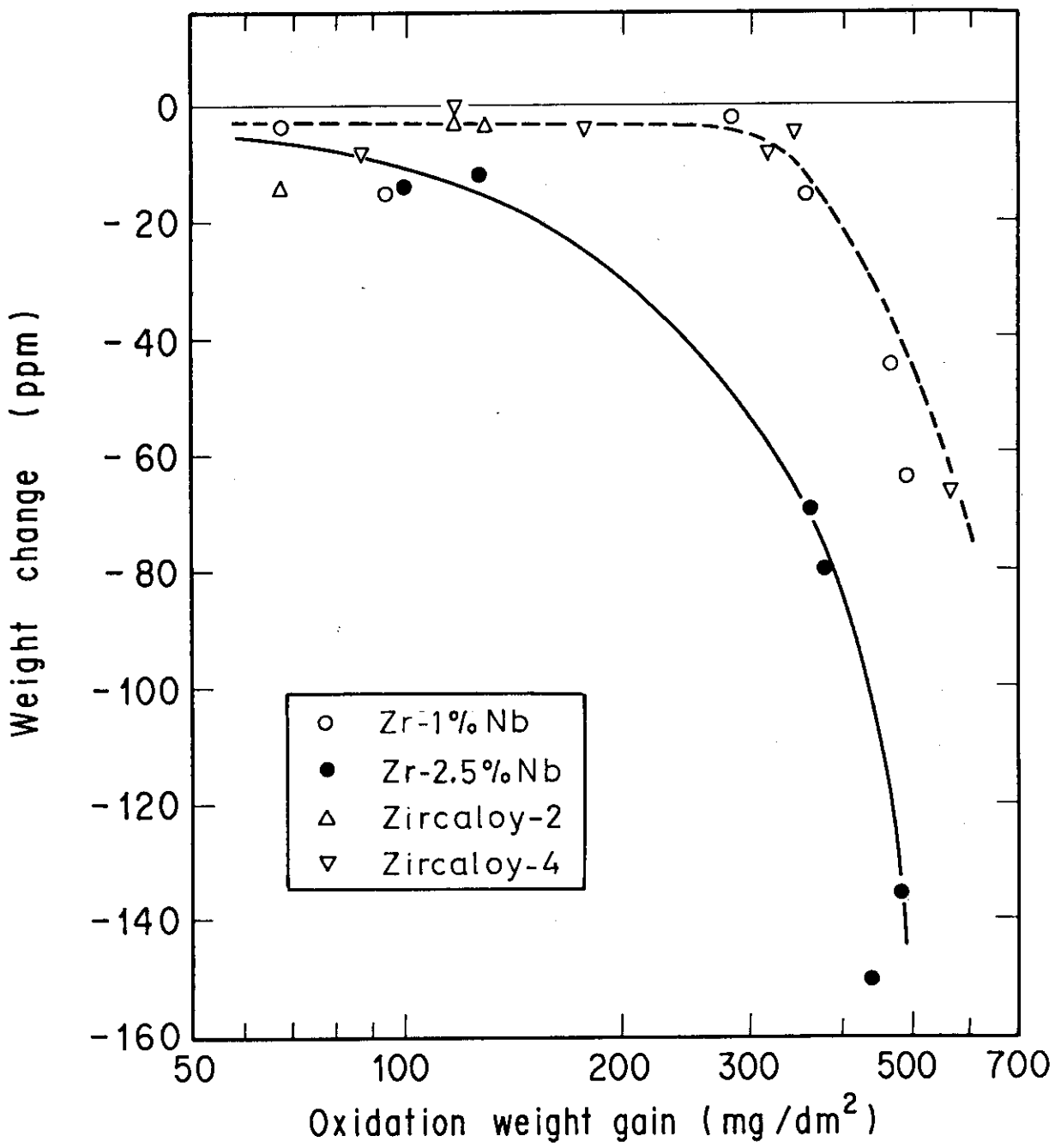

Fig. 15 Weight reduction against prior oxidation level (pre-oxidized in oxygen and then hydrided)